Electronic Structure I Mark Pederson, Chairman

Properties of incommensurate spin density waves in iron aluminides (invited)

D. R. Noakes
Center for Interactive Micromagnetics, Virginia State University, Petersburg, Virginia 23806

A. S. Arrott
Center for Interactive Micromagnetics, Virginia State University, Petersburg, Virginia 23806 and MSEL, National Institute of Standards and Technology, Gaithersburg, Maryland 20899

M. G. Belk
Center for Interactive Micromagnetics, Virginia State University, Petersburg, Virginia 23806

S. C. Deevi
Research, Development and Engineering Center, Philip Morris USA, Richmond, Virginia 23261

J. W. Lynn
NCNR, National Institute of Standards and Technology, Gaithersburg, Maryland 20899

R. D. Shull
MSEL, National Institute of Standards and Technology, Gaithersburg, Maryland 20899

D. Wu
Thayer School of Engineering, Dartmouth College, Hanover, New Hampshire 03755

(Presented on 6 January 2004)

Neutron diffraction in Fe(Al) reveals incommensurate spin density waves (SDWs) in alloys known to be spin glasses. The wave vectors for crystals of Fe(34Al), Fe(40Al) and Fe(43Al) show n varying from 11 to 6 for $\mathbf{q}=2\pi(h\pm 1/n,k\pm 1/n,l\pm 1/n)/a_o$, where (h,k,l) and a_o characterize the parent bcc lattice of the CsCl structure. The magnetic reflections are present far above the spin-glass freezing temperatures. These SDWs keep the spins on nearest-neighbor Fe atoms close to parallel, in contrast with SDWs in Cr, which keep nearest-neighbor spins close to antiparallel. The competition between near-neighbor Fe–Fe ferromagnetism and 180° superexchange through the Al site has been used to explain the spin-glass behavior, but the appearance of the SDWs calls for a more fundamental source of the periodicity. The phase shift mechanism for SDW interactions with magnetic moments is invoked to explain the breadth of the peaks, which resemble the results for Cu(Mn), Pd(Mn), and Pd(Cr). The data are interpreted using cubic symmetry, but it has yet to be established whether the wave vectors all occur in a single domain or whether there are multiple domains. There are 48 wave vectors of magnitude almost equal to the {110} wave vectors of the bcc lattice, which could stabilize the SDWs by spanning the Fermi surface. These unanticipated results should have pervasive ramifications for the theory of metallic magnetism. © *2004 American Institute of Physics.* [DOI: 10.1063/1.1667415]

I. INTRODUCTION

The iron–aluminides serve as a testing ground for the inadequacies of the local spin density approximation (LSDA), as well as the attempts to make up for these using the generalized gradient approximations.[1,2] LSDA has some serious problems in trying to account for such basic problems as the ground state of chromium[3,4] and iron.[5–7] It seems likely that this is related to systems that do not have well-defined local magnetic moments.[8,9] Whether iron–aluminides have moments that exhibit a local thermodynamic spin degree of freedom is an open question. It is possible that our recent discovery[10] by neutron diffraction of incommensurate spin density waves (SDWs) in Fe–Al alloys with aluminum concentrations between 32% and 50% may provide the impetus to those who would go beyond the LSDA to describe the exchange energy as the nonlocal interaction that it is.

The diffraction results, taken to date from the National Institute of Standards and Technology Center for Neutron Research, leave many unanswered questions, some as basic as the symmetry of the magnetic structure. Figure 1 shows an intensity contour plot of two SDW satellites observed around the origin in Fe(43Al) at 1.5 K. The (small) difference in intensity may be due merely to sample and diffraction geom-

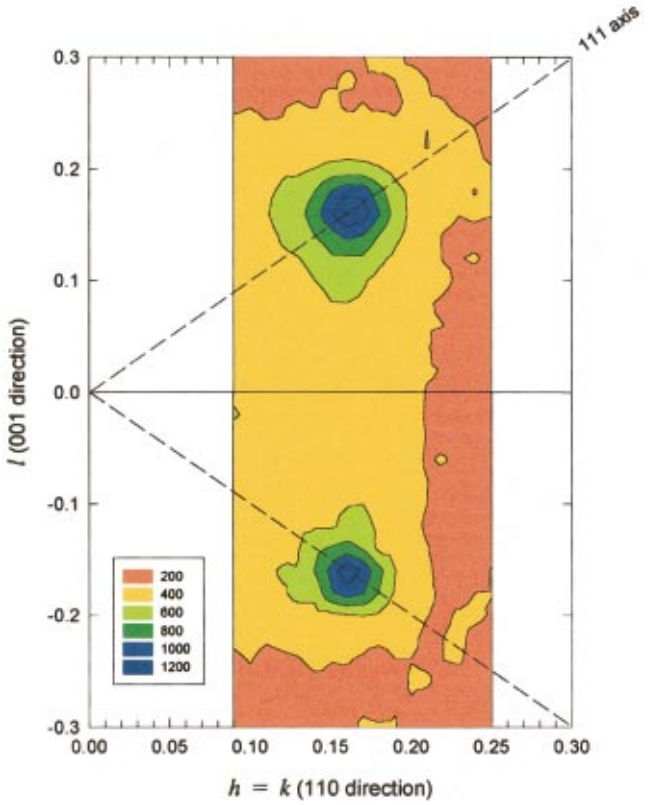

FIG. 1. (Color) Contour plots of the diffraction intensity near the origin for Fe(43Al) at 1.5 K, showing an incommensurate structure at $(1/n,1/n, \pm 1/n)$ for $n=6$.

etry. Similar satellites have been observed around the origin (110) and (002) positions, but not around (001) or (111). The results can be described as arising from a set of magnetic reflections in reciprocal lattice space given by

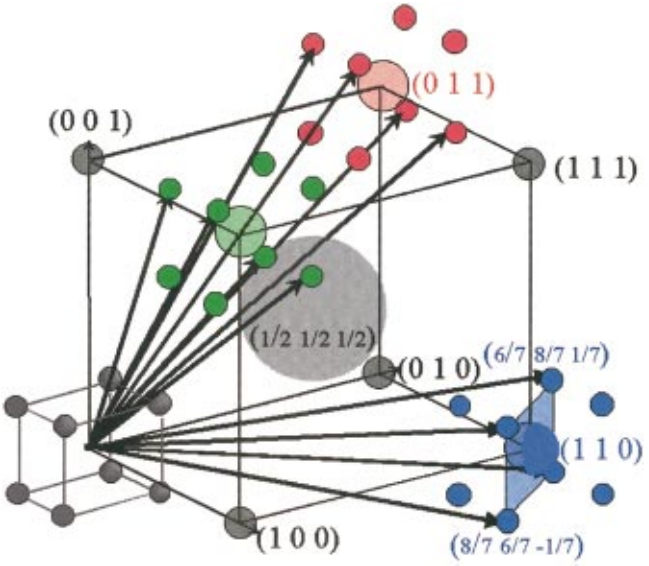

FIG. 2. (Color) Reciprocal space positions of SDW satellites observed in Fe–Al alloys. The gray area around $(\frac{1}{2},\frac{1}{2},\frac{1}{2})$ indicates weak temperature-independent Fe_3Al structural correlations on a fcc lattice corresponding to Fe_9Al_7.

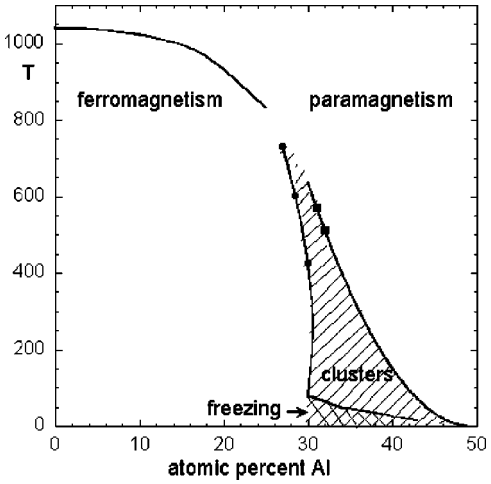

FIG. 3. A speculative magnetic phase diagram for the iron–aluminum system ignoring the effects of ordering on the Al simple cubic lattice complex. The cluster region was postulated by Okamoto (see Ref. 18) based on his high temperature susceptibility measurements for the alloys for which points are shown. The freezing temperatures are taken from the work of Shull, Okamoto, and Beck, (see Ref. 12) and Takahashi, Li, and Chiba (see Ref. 28). A quadratic dependence on the number of Fe atoms on the Al simple cubic lattice complex was assumed to give the upper-limit temperature of the cluster region.

$$\mathbf{q}=\frac{2\pi}{a_o}\left(h\pm\frac{1}{n},k\pm\frac{1}{n},l\pm\frac{1}{n}\right), \tag{1}$$

where n varies continuously with concentration of Al, a_o is the lattice parameter and (h,k,l) refer to the underlying bcc lattice of these alloys with the B2(CsCl) structure. The way the **q** vectors are expressed in Eq. (1) could imply cubic symmetry with eight reciprocal lattice vectors about each of the lattice reflections of the parent bcc lattice. This is shown in Fig. 2. But this may not be the case. With the application of fields or strains the intensity of the eight spots might become unequal, indicating a domain structure with different **q** vectors being favored in each domain.

The B2 structure of the iron–aluminides in this composition range is composed of two lattice complexes, each of which is simple cubic. Nearest neighbors of one simple cubic lattice complex are all on the other simple cubic lattice com-

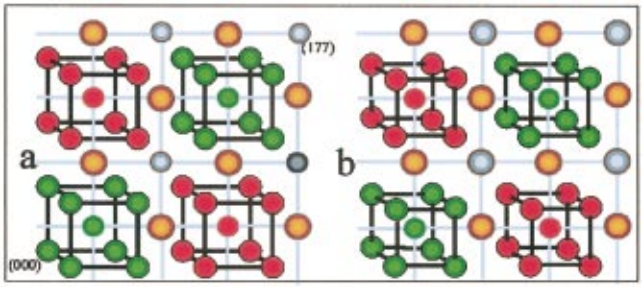

FIG. 4. (Color) Magnetization patterns with cubic symmetry for (a) Fe_3Al, and (b) Fe_9Al_7. The green and red atoms are Fe(II) sites with opposite spin directions. The gold atoms are Al. The gray atoms sit in positions of magnetic frustration. In (a) these are Fe(I) and in (b) they are Al. The first three layers of the 128 atom cubic unit cells are shown in perspective. The Fe(II) sites in (a) are fixed at $\frac{1}{4}\frac{1}{4}\frac{1}{4}$, but in (b) the position is adjustable along the diagonal.

plex. These are labeled (I) and (II), where (II) is occupied by only Fe atoms, while (I) has random occupation of Fe and Al atoms. For stoichiometric FeAl, the occupancy of the two sites is exclusive, except for effects of defects and the occurrence of vacancies. Away from stoichiometry there is a tendency of the random occupation not to be completely random. This leads to the formation of the DO3 structure associated with Fe_3Al for concentrations of Al below 30 at. %. For the DO3 structure, there are four interpenetrating face-centered-cubic lattice complexes. At the stoichiometric composition of Fe_3Al, one of these has all the aluminum, one has Fe(I) atoms with only Fe nearest neighbors and two have Fe(II) atoms with equal numbers of Fe and Al neighbors. It has long been speculated that the moment on the Fe atom depends on the local environment. Indeed early neutron diffraction results on Fe_3Al ascribe 2.2 μ_B to the Fe(I) atoms that are surrounded by Fe(II) atoms and only 1.8 μ_B to the Fe(II) atoms.[11] From measurements of the saturation magnetization and from Mössbauer studies, it has been possible to numerologically assign various moments to various configurations.[12,13] The fact that iron–aluminides can be disordered by mechanical means to obtain ferromagnetic materials emphasizes the effect of environment on the local moment.[14] We report below the results of applying high fields to an Fe(34Al) alloy, which may be interpreted as showing a field-induced moment.

The local moment questions are important to the understanding of the incommensurate spin density waves seen in the iron–aluminides. Does the molecular field, arising from the spin density wave, act to align moments, does it induce the moments, or is it a mixture?

Grest[15] pointed out in 1980 that Fe_3Al would give the cubic structure in reciprocal lattice space of Eq. (1) with $n=4$, if magnetic interactions were dominated by the 180° superexchange between Fe(II) atoms on diagonally opposite corners of a bcc unit cell through the Al atom at the center of the cell. But Fe_3Al is ferromagnetic because the 180° superexchange is not sufficiently strong. Such an interaction had been invoked by Sato and Arrott[16] to explain their results[14] for the magic composition Fe(30.5Al), where the material goes from paramagnetic at high temperatures to ferromagnetic at intermediate temperatures and then back to paramagnetic (or superparamagnetic, or mictomagnetic) at lower temperatures and then to some antiferromagnetic-like order at the lowest temperatures. The model of Sato and Arrott was presented before the subject of spin glasses was developed. They predicted ordinary antiferromagnetism at low temperatures, but this was not observed by neutron diffraction.[11] Subsequently the results of magnetic measurements on iron–aluminides have been interpreted as showing spin glass behavior at low temperature in addition to some interesting micromagnetic cluster effects at temperatures for which ferromagnetism might have been expected on the basis of the results for lower concentrations.[17] All this is reflected in the speculative diagram shown in Fig. 3 using the results of Okamoto[18] who first suggested the cluster region from analysis of high temperature susceptibility. The reentrant behavior at 30.5 at. % Al has yet to be explained. The competition between near-neighbor ferromagnetic coupling and third-neighbor antiferromagnetic coupling through an Al atom has a firm theoretical basis. The superexchange interaction appears in cluster calculations of Reddy *et al.*[19]

The model of Grest would apply to the hypothetical ordered structure Fe_9Al_7,[20] shown in Fig. 4. The symmetry of Fe_9Al_7 differs from that of Fe_3Al in that the position of the Fe(II) atoms is restrained to coordinates $\frac{1}{4},\frac{1}{4},\frac{1}{4}$ in Fe_3Al but not in Fe_9Al_7. This allows the volume per Fe atom to be variable even with fixed lattice constant. Thus the moment of the Fe atom could change with the coordinates of its position. This is important to remember in thinking about the B2 structure with its random positions of Fe(I) atoms influencing the volume and moments of the Fe(II) atoms. The magnetic structure of Fe_9Al_7 could be that of Eq. (1) with $n=8$, as shown in Ref. 10. The existence of some local antiferromagnetic interaction is a prerequisite for obtaining spin-glass behavior. That this occurs when Fe atoms interact through Al atoms even in such a dilute magnetic system as $FeAl_2$[21] illustrates the importance of exchange through the Al atoms. One might wonder if the competition between the ferromagnetic interactions of nearest-neighbor Fe atoms and 180° superexchange across the body diagonal would be sufficient to account for the neutron diffraction observations in the B2 structure with its disorder on the Al simple cubic lattice complex, or is it necessary to invoke an Overhauser instability in the electron gas of the conduction electrons[22] to explain the results? It is this latter question that pertains to the current interests in the application of LSDA to the metallic magnetism in the first transition series.

This work is made possible by substantial improvements in the metallurgy of iron aluminides. The polycrystalline samples of Fe(40Al) are extremely homogeneous alloys developed for commercial applications starting from fine powders created by gas quenching from the molten state.[23] Single crystals of iron aluminides were prepared for detailed metallurgical studies of the magnetic decoration of dislocations.[24]

II. DETAILS OF THE NEUTRON DIFFRACTION RESULTS

The first thing to note about the neutron diffraction results is that this is not Cr. In bcc Cr the spins on the cube corners are aligned oppositely to those on the cube centers. The structure is generated by a wave vector that is not quite $(100)2\pi/a_o$, leading to a modulation of the structure with the moments on the corners and centers reversing over a distance of the order of 14 cubic cells. In the iron–aluminides the spins on the cube corners are aligned parallel to those on the cube centers. The structure is generated by wave vectors that are not quite (110) (Fig. 2) leading to a modulation of the ferromagnetism: the moments on the corners and centers reversing over a distance of the order of n cubic cells, where n is the number in Eq. (1). Cr is a variation on antiferromagnetism. The iron–aluminides are variations on ferromagnetism. Unlike Cr, the magnetic reflections are not sharp; see Fig 5. This can result from the appearance of a very fine domain structure or it can be due to a gradual readjustment of the phase of the spin density wave to take into account the local arrangement of Fe atoms. The latter is

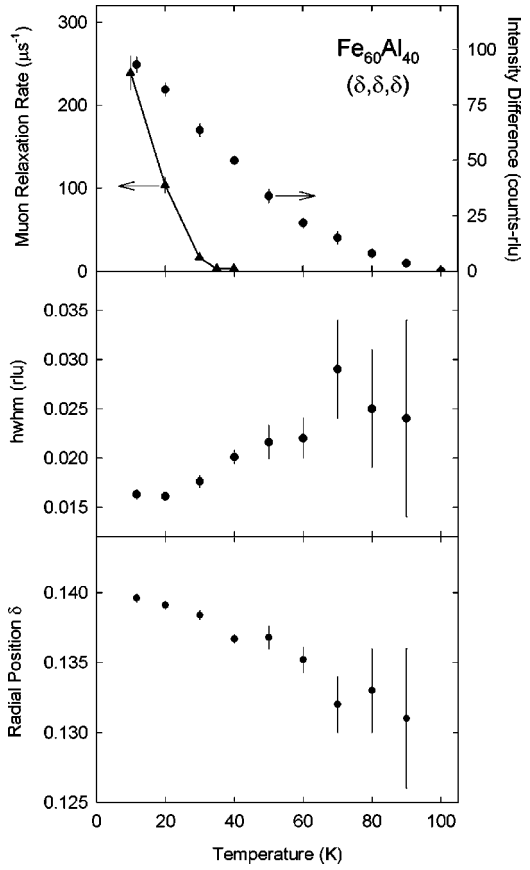

FIG. 5. Temperature dependence of Fe(40Al) properties: (a) the integrated peak intensity for the $(1-\delta,1-\delta,\delta)$ reflection extracted from the difference between radial scans at the temperatures shown and a scan at 100 K (the zero is thus not absolute), (b) the half width at half maximum for the peak, (c) the mean value of $\delta\ (=1/n)$. The temperature dependence of the muon relaxation rate in the homogeneous polycrystalline material is shown in (a) for comparison.

called the phase-shift mechanism, used to explain magnetization results in single crystals of Cu(Mn) alloys.[25,26]

From the polycrystalline Fe(40Al) diffraction data, we can put a lower bound on the moment per atom if we take as a model the extreme case of a single **q** state with a transverse helical SDW. This yields a moment of 0.26 μ_B per atom if every atom (Fe and Al) were to carry the same moment. The decrease in moment with increasing Al, seen in the single crystals, has yet to be quantified.

Like the spin density waves in Cu(Mn) alloys,[27] the temperature dependence shown in Figs. 5 and 6 appears to be more gradual than that expected from an antiferromagnetic transition at the ''spin-glass temperature,'' where there is a pronounced maximum in the Fe(Al) ac susceptibility.[12,28] These results were interpreted in Ref. 10 by having the moments respond to a temperature independent applied field with the periodicity of Eq. (1), plus a self-interaction term. In the analysis of Fig. 6, we assume only the periodic applied field. The spin freezing is at low temperature relative to any onset of the SDW, which causes the periodic applied field that clearly persists well above 100 K in our data. Although, in our experiments, there is no indication of the spin-glass freezing temperature, in the work of Gotaas, Rhyne and Werner[27] on Cu(Mn), they were able to see the spin-glass

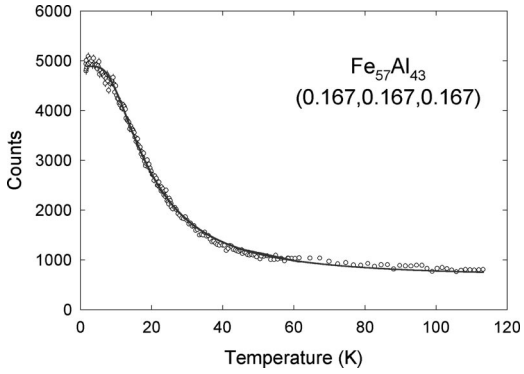

FIG. 6. Temperature dependence of counts (per 4 min) at a location very near the maximum of the (δ,δ,δ) SDW scattering peak in Fe(43Al). The solid line is a least squares fit of a model of spin $\frac{1}{2}$ moments in a temperature-independent periodic field, with a characteristic temperature of 17 K. Even at the highest temperature measured, the signal is still 150 counts above background. If the model is correct, it implies the existence of the SDW at temperatures well above the range of measurement.

freezing temperature by going to extremely tight 0.006 meV resolution. The energy resolution of our experiments is 1 meV, or 0.25 THz. This implies that we are observing slowly moving ''spin density wave clouds'' as suggested by Hicks and Cable[29] to describe not only Cu(Mn) but also Pd(Mn) and Pd(Cr). To provide a view on a longer time scale, we used muon spin relaxation measurements. The muon work that provided the impetus to look once again by neutrons is described below.

III. HIGH FIELD MAGNETIC SUSCEPTIBILITY

The magnetization of the Fe(34Al) crystal has been measured from 300 to 5 K in fields to 5 T. The results are shown in Fig. 7. The magnetization in 5 T is weakly temperature dependent as shown at the top of Fig. 7. The field depen-

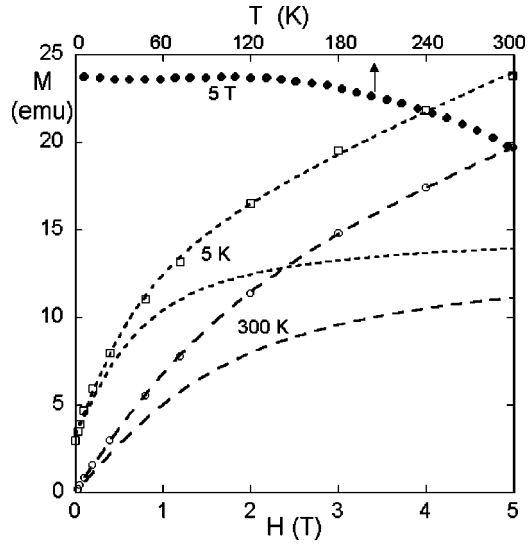

FIG. 7. The magnetization of the Fe(34Al) crystal from 300 to 5 K in fields coming down from 5 T (upper curve for each of the two temperatures shown). The magnetization in 5 T is weakly temperature dependent as shown at the top. An analysis yields a saturating component (lower curves) and a component that remains linear with field to at least 5 T at each temperature.

dence can be analyzed to yield a saturating component and a component that remains linear with field to at least 5 T. Almost all of the weak temperature dependence is in the observation that the saturating component at 5 K saturates at half the field as the saturating component at 300 K. The magnetization at 5 K shows a remanence on reducing the field from 5 T. The hysteresis loop closes gradually as the field is reversed to -5 T. This reflects some of the spin-glass properties of this material, but it is clear that the main cluster phenomena are present at 300 K and above as suggested by Okamoto.[18] The peak in the temperature dependence of the the ac susceptibility, which denotes the onset of spin-glass freezing below 35 K, is a minor effect on the scale of the changes in magnetization with field and temperature. The large linear term in the susceptibility suggests field-induced moments.

IV. MUON SPIN RELAXATION

Muon spin relaxation (μSR) is a local probe of interstitial hyperfine fields in materials. In it, polarized positive muons produced at an accelerator laboratory are stopped in the sample of interest. Each muon's magnetic moment precesses around the local field at the muon site during each muon's lifetime there, and then the moment direction at the instant of decay is signaled by the direction of motion of the decay positron (a parity-violating decay, $\tau_\mu \cong 2.2\ \mu$s). Fast electronics measure the time between each muon's arrival and the departure of its decay positron, and large numbers of decay-time and positron-direction ''events'' are tabulated. In zero applied field (ZF), these are collected into two histograms: events ''forward'' and ''backward'' (with respect to the initial polarization) as a function of time, over several muon lifetimes. The muon ensemble polarization as a function of time is proportional to the directional asymmetry in the events, which is extracted as the difference between the histograms divided by their sum (after some instrumental corrections). For reviews, see Refs. 30 and 31.

ZF-μSR was measured at the Paul Scherrer Institute in part of the polycrystalline Fe(40Al) sample for which neutron scattering was reported in Ref. 10. The muon spin relaxation function was exponential with relaxation rate near $0.34\ \mu s^{-1}$ at 60 K and higher temperatures. Such exponential relaxation is usually indicative of a rapidly fluctuating local field at each muon site. Since muons are unlikely to be diffusing in this temperature range in a random-alloy material such as this, the fluctuating local field is most likely due to coupling to fluctuating atomic spins. Since there is no significant variation with temperature above 60 K, this may be the ''paramagnetic limit,'' where the moment fluctuation rate has reached the maximum value allowed by the exchange coupling in the material.

When material with a simple crystal structure enters a simple long-range magnetic-ordering structure, the ordering will normally generate a unique magnetic field magnitude, or a small number of distinct field values, at the muon site, slowly fluctuating relative to any paramagnetic electronic fields coupled to the muon in the paramagnetic state. In the static, unique-field limit, all muons will precess at the same frequency, generating ''spontaneous oscillation'' in the ZF asymmetry spectra. This is what happens in pure iron. For progressively more complicated or disordered magnetic states, or with fluctuations, sharp frequencies broaden into average frequencies with ''linewidths'' generating relaxation: the oscillations develop an envelope that relaxes to zero size. If the disorder and fluctuations become large enough, all direct evidence of coherent oscillation is lost, and the asymmetry spectrum only shows monotonic relaxation to zero. If this relaxation is significantly faster than in the paramagnetic state, then it still provides information on (disordered) magnetic freezing. We do not see spontaneous oscillations in ZF-μSR from Fe(40Al), but we do see increased relaxation at lower temperatures.

The relaxation rate begins to rise as temperature drops below 60 K, and the shape of the relaxation function changes gradually. From 45 down to 10 K (the lowest temperature measured), the relaxation can be fit as the sum of two exponentials, with the faster exponential increasing in amplitude at the expense of the slower exponential as temperature decreases. This is consistent with an inhomogeneous freezing process, often seen in μSR of concentrated-moment spin glasses. The fractional amplitude of the faster-relaxing signal indicates the fractional volume of the sample that is in the frozen state; for Fe(40Al) this rises from near zero above 45 K to 100% at 20 K. Meanwhile the relaxation rate of the faster exponential signal rises dramatically as temperature is reduced, as shown in the upper panel of Fig. 5. This rate is so large at 20 K and below that much of the initial muon ensemble polarization is lost in the histogram initial dead time (about 10 ns). This also is often seen in μSR of concentrated spin glasses: it indicates significant frozen moments (at least several tenths of a Bohr magneton per Fe). The loss of initial relaxation in the dead time means that the true shape of the static-limit relaxation function at low temperatures cannot be seen in this sample. We hope to be able to see it in μSR of samples closer to 50% Al concentration.

It is interesting that the temperature dependence of the muon spin relaxation bears little resemblance to the temperature dependence of the neutron diffraction from the same sample. In neutron diffraction, the intensity of the low-angle SDW peak begins to rise as temperature drops below ~ 110 K, and is rising most rapidly near 50 K, the range where the μSR signal just begins to have temperature dependence. The difference is due to the different frequency ranges of the two probes' sensitivity to dynamics. Neutron scattering detects vibrations in THz, while μSR detects fluctuations in the range of MHz to GHz. With typical neutron spectrometers, such as the diffractometer used for Fe(40Al), vibrations and fluctuations at less than a few tenths of a THz contribute to the ''quasi-elastic'' peak, and are not resolved from the elastic (static scatterer) peak. Thus, while neutron-static SDW ordering begins to increase as temperature drops below 110 K in this sample, the μSR results indicate the magnetic moments are still fluctuating at rates at least in the high GHz range until temperatures get below 60 K. The muon spin relaxation remains typical of dynamic local fields down to 20 K, but there is indication in the small resolved signal at 10 K that the fields at that temperature are at last

muon static (fluctuation rates less than ~ 1 MHz). Combination of the temperature dependence of the two probes thus indicates that the spin-freezing process is quite gradual with temperature. This echoes our analysis of the temperature dependence of the SDW intensity, which is not consistent with a sharp freezing ''transition,'' needing instead some effective field persisting to perhaps 500 K.

V. CONCLUSION

This work has just begun. We expect it to be at least as interesting as the ongoing Cr saga. We do not know whether there is indeed cubic symmetry from multiple q's in each region or lowered symmetry from single q states in multiple regions. Nothing has been learned yet about polarization axes. We have yet to carry out such tasks as finding the effects of magnetic fields, pressure, strains and changes in alloy composition by substitution of other atoms. As little as 0.5 at. % B has dramatic effects on the stacking faults in Fe(40Al).[32] The role of ordering of the iron atoms on the Al cubic lattice complex should be considered in light of Fig. 4, showing how a well atomically ordered material might behave and the observation of some additional ordering in broad diffraction peaks about the $\frac{1}{2}\frac{1}{2}\frac{1}{2}$ positions. Heat capacity measurements would show whether the moments on the Fe atoms have a thermodynamic spin degree of freedom or result from a more itinerant electron model.[9]

There is a vast literature on the iron–aluminides, with much discussion by theorists, experimentalists and technologists. Recent theoretical discussion has concentrated on crystal structure, ferromagnetism and paramagnetism. The appearance of static spin density waves in iron–aluminides raises additional experimental and theoretical questions. These unanticipated results should have pervasive ramifications for the theory of metallic magnetism.[33]

Note added in proof: In their literature search the authors missed the extensive neutron diffraction studies of Shapiro and co-workers[34–37] on $Fe_{0.7}Al_{0.3}$ showing, among many other things, the appearance of a ''field-induced modulated structure in the reentrant spin glass $Fe_{70.4}Al_{29.6}$ in applied magnetic fields.''[34] The field turns the net magnetization of the clusters toward the direction of the scattering vector, rendering it invisible to neutron scattering and revealing the underlying peak corresponding to $n=12$ in Eq. 1. The present work on higher Al concentrations supports their conjecture that a SDW is the most promising among a number of possible explanations for this effect in the highly complex $Fe_{0.7}Al_{0.3}$ iron-aluminide.

ACKNOWLEDGMENTS

The Center for Interactive Micromagnetics of Virginia State University is directed by Professor C. E. Stronach and supported by the U.S. Air Force Office of Scientific Research Grant No. F49620-00-1-0364.

[1] F. Lechermann, F. Welsch, C. Elsasser, C. Ederer, M. Fahnle, J. M. Sanchez, and B. Meyer, Phys. Rev. B **65**, 132104 (2002).
[2] S. Kurth, J. P. Perdew, and P. Blaha, Int. J. Quantum Chem. **75**, 889 (1999).
[3] P. M. Marcus, S. L. Qui, and V. L. Moruzzi, J. Phys.: Condens. Matter **10**, 6541 (1998).
[4] R. Hafner, D. Spisak, R. Lorentz, and J. Hafner, Phys. Rev. B **65**, 184432 (2002).
[5] G. Y. Guo, H. Ebert, W. M. Temmerman, K. Schwarz, and P. Blaha, Solid State Commun. **79**, 121 (1991).
[6] J. Zhu, X. W. Wang, and S. G. Louie, Phys. Rev. B **45**, 8887 (1991).
[7] M. Fähnle, M. Komelj, R. Q. Wu, and G. Y. Guo, Phys. Rev. B **65**, 144436 (2002).
[8] D. A. Papaconstantopoulos and K. B. Hathaway, J. Appl. Phys. **87**, 5872 (2000).
[9] D. A. Papaconstantopoulos, I. I. Mazin, and K. B. Hathaway, J. Appl. Phys. **89**, 6889 (2001).
[10] D. R. Noakes, A. S. Arrott, M. G. Belk, S. C. Deevi, Q. Z. Huang, J. W. Lynn, R. D. Shull, and D. Wu, Phys. Rev. Lett. **91**, 217201 (2003).
[11] S. J. Pickart and R. Nathans, Phys. Rev. **123**, 1163 (1961).
[12] R. D. Shull, H. Okamoto, and P. A. Beck, Solid State Commun. **20**, 836 (1976).
[13] J. W. Cable, L. David, and R. Para, Phys. Rev. B **16**, 1132 (1977).
[14] A. Arrott and H. Sato, Phys. Rev. **114**, 1420 (1959).
[15] G. S. Grest, Phys. Rev. B **21**, 165 (1980).
[16] H. Sato and A. Arrott, Phys. Rev. **114**, 1427 (1959).
[17] S. M. Shapiro, in *Spin Waves and Magnetic Excitations*, edited by A. S. Borovik-Romanov and S. K. Sinha (Elsevier, New York, 1988), Vol. 2, p. 219.
[18] H. Okamoto, Ph.D. thesis, University of Illinois, 1971.
[19] B. V. Reddy, S. C. Deevi, F. A. Reuse, and S. N. Khanna, Phys. Rev. B **64**, 132408 (2001).
[20] G. P. Das, B. K. Rao, P. Jena, and S. C. Deevi, Phys. Rev. B **66**, 184203 (2002).
[21] C. S. Lue, Y. Öner, D. G. Naugle, and J. H. Ross, Phys. Rev. B **63**, 184405 (2001).
[22] A. W. Overhauser, Phys. Rev. **128**, 1437 (1962).
[23] S. C. Deevi, Intermetallics **8**, 679 (2000).
[24] D. Wu and I. Baker, Mater. Sci. Eng., **A329–331**, 334 (2002).
[25] B. R. Coles and A. Arrott, J. Appl. Phys. **32**, 51S (1961).
[26] A. Arrott, in *Magnetism* edited by H. Suhl and G. T. Rado (Academic, New York, 1966), Vol. IIIB.
[27] J. A. Gotaas, J. J. Rhyne, and S. A. Werner, J. Appl. Phys. **57**, 3404 (1985).
[28] S. Takahashi, X. G. Li, and A. Chiba, J. Phys.: Condens. Matter **8**, 11243 (1996).
[29] T. J. Hicks and J. W. Cable, Phys. Rev. B **58**, 5177 (1998).
[30] A. Schenck and F. N. Gygax, in *Handbook of Magnetic Materials*, edited by K. H. J. Buschow (Elsevier, Amsterdam, 1995), Vol. 9, p. 57.
[31] G. M. Kalvius, D. R. Noakes and O. Hartmann, in *Handbook on the Physics and Chemistry of Rare Earths*, edited by K. A. Gschneidner, L. Eyring, and G. H. Lander (Elsevier, Amsterdam, 2001), Vol. 32, p. 55.
[32] L. Pang and K. S. Kumar, Acta Metall. **49**, 2215 (2001).
[33] K. Capelle and L. N. Oliveira, Phys. Rev. B **61**, 15228 (2000).
[34] P. Boni, S. M. Shapiro, and K. Motoya, Solid State Commun. **60**, 881 (1986).
[35] S. Raymond, W. Bao, S. M. Shapiro, and K. Motoya, Physica B **241–243,** 597 (1998).
[36] W. Bao, S. Raymond, S. M. Shapiro, K. Motoya, B. Fåk, and R. W. Erwin, Phys. Rev. Lett. **82**, 4711 (1999).
[37] S. M. Shapiro, W. Bao, S. Raymond, S. H. Lee, and K. Motoya, Appl. Phys. A **74** [Suppl.] S-859 (2002).